Electronic Supplementary Material (ESI) for Journal of Materials Chemistry A.
This journal is © The Royal Society of Chemistry 2018

Supporting Information (SI) for:

Electrochemically Activated Cobalt Nickel Sulfide for Efficient Oxygen Evolution Reaction: Partial Amorphization and Phase Control

Yu-Rim Hong[1,2,†], Sungwook Mhin[3,†], Kang-Min Kim[1,†], Won-Sik Han[2], Heechae Choi[4,5], Ghulam Ali[6], Kyung Yoon Chung[6], Ho Jun Lee[1], Seong-I Moon[7], Soumen Dutta[7], Taeseup Song[7,*], HyukSu Han[1,*]

[1]*Korea Institute of Industrial Technology, 137-41 Gwahakdanji-ro, Gangneung-si, Gangwon 25440, Republic of Korea*

[2]*Department of Chemistry, Seoul Women's University, Seoul, Republic of Korea*

[3]*Korea Institute of Industrial Technology, 156 Gaetbeol-ro, Yeonsu-gu, Incheon 406-840, Republic of Korea*

[4] *Institute of Inorganic Chemistry, University of Cologne, 50939 Cologne, Germany*

[5]*Institute of Inorganic Chemistry, University of Cologne, Greinstr. 6, 50939, Cologne, Germany*

[6]*Center for Energy Convergence Research, Korea Institute of Science and Technology, Hwarang-ro 14-gil 5, Seongbuk-gu, Seoul 02792, Republic of Korea*

[7]*Department of Energy Engineering, Hanyang University, Seoul 04763, Republic of Korea*

Experimental Section

Electrochemical Measurements: The electrochemical performance of catalysts in 1 M KOH was evaluated using a standard three-electrode electrochemical cell with a rotating disk electrode (RDE) configuration controlled by an electrochemistry workstation (model Autolab PGSTAT; Metrohm). For the preparation of the working electrode, a sample (4 mg) was dispersed in a Nafion® solution (30 µL, 5 wt%) of water (1 mL) and ethanol (volume ratio 3:1). A homogeneous ink formed after sonicating overnight. Then, the as-prepared catalyst ink (5 µL) was drop-cast onto the surface of a glassy carbon (GC) RDE electrode having a diameter of 3 mm, yielding an approximate catalyst loading of 0.285 mg cm^{-2}. The working electrode was dried overnight prior to electrochemical measurements. The electrolyte was purged with O_2 before measurements. During the measurements, the RDE electrode was rotated constantly at 2,000 rpm to remove bubbles. $Hg|Hg_2SO_4$ and graphite rod were used as the reference electrode and counter electrode, respectively. Linear sweep voltammetry (LSV) was conducted at a scan rate of 5 mV s^{-1} from 1.23 to 2.0 V vs. reversible hydrogen electrode (RHE). The potentials were calibrated against RHE and all polarization curves were *iR*-compensated.

Cyclic voltammetry (CV) was used to measure the electrochemical effective surface area (EESA). The test was performed in an O_2-saturated 1 M KOH solution to estimate the electrochemical double-layer capacitance (C_{dl}) at non-Faradaic overpotentials. A series of CV measurements were conducted at various scan rates (20, 40, 60, 80, 100, and 120 mV s^{-1}) ranging from 1.41 to 1.46 V vs. RHE. The difference in current density between the anodic and cathodic sweeps (J_{anodic}–$J_{cathodic}$) at 1.435 V vs. RHE was plotted as a function of the scan rate; the slope was equal to twice the C_{dl} of the catalyst. Electrochemical impedance spectroscopy (EIS) was performed over the frequency range of 0.1–100 kHz under the applied voltage where the current density reached ca. 10 mA cm^{-2}. A sinusoidal voltage with amplitude of 5 mV was applied during the measurements. The resulting impedance data were then fitted using the Randles equivalent circuit model. Faradaic efficiency (FE) of ECA-CNS was measured by using a rotating ring disk electrode (RRDE). A ring potential of 0.4 V_{RHE} was applied to detect O_2 molecules generated by oxygen reduction reaction (ORR). A constant current of 0.48 mA was applied to the disk electrode for O_2 generation, and then FE of CNS-NGA was calculated using the following equation.

$$FE = i_{ring} / (i_{disk} \times N) \tag{1}$$

where, idisk, iring, and N denote the disk current, the ring current, and the current collection efficiency of the RRDE which is generally about 0.2.

Electrochemical Activation**:** 4 mg of the powder was dispersed in a Nafion® solution (30 μL, 5 wt%) of water (1 mL) and ethanol (volume ratio 3:1). A homogeneous ink formed after sonicating overnight. Then, the as-prepared catalyst ink was drop-cast onto florinde doped tin oxide (FTO) glass substrate. The FTO electrode is dried at room temperature for overnight. Electrochemical activation process is performed in 1 M KOH solution using a standard three-electrode electrochemical cell controlled by an electrochemistry potentiostat (model Autolab PGSTAT; Metrohm). The FTO electrode was used as working electrode, and Ag|AgCl (3.5 M KCl) and graphite rod were used as the reference and counter electrodes, respectively. 1.55 V against a reversible hydrogen electrode (RHE) was applied to working electrode until the current saturation occurs.

X-ray Absorption Spectroscopy: X-ray absorption spectroscopy (XAS) was performed at Co and Ni K-edge of CNS-rGO and Ni_2CoS_4 using a Si (111) double-crystal monochromator at the 1D, 7D, and 8C beamlines of Pohang light source (PLS-II) South Korea. High-order harmonics was eliminated by adjusting the monochromator. The data were collected in transmission mode after eliminating the high-order harmonics by adjusting the monochromator.

Reference spectra of Co and Ni were also collected simultaneously with each measurement for energy calibration. In order to compare the Co K-edge spectra of CNS-rGO and Ni2CoS4, X-ray absorption near edge structure (XANES) spectra of CoO and $LiCoO_2$ was also measured plotted. Similarly, XANES spectra of NiO and $LiNiO_2$ was also to compare the Ni K-edge spectra of both materials. The extended X-ray absorption fine structure (EXAFS) data was extracted with weighted by k^2 in k-ranges of 2.0 ~ 11 $Å^{-1}$ (Co edge) and 2.0 ~ 10 $Å^{-1}$ (Ni edge) using Hanning window function. Fourier transform (FT) data were converted without phase corrected and fitted using theoretical crystal structure information. EXAFS spectra were fitted in the *R*-range of up to 4.0 Å using theoretically generated scattering paths of Ni_2CoS_4 (98-062-4474) and $CoNiS_2$ (ICDD 98-602-4479) structures. The amplitude reduction factor was determined from the initial fitting session and fixed to 0.89 during fitting of EXAFS data. All the XAS data was processed using Athena and Artemis programs.[1]

Density Functional Theory Calculations: Density functional theory (DFT) calculations were performed using the generalized gradient approximation (GGA) with Perdew–Burke–Ernzerhof (PBE) parameterization[2] and the Vienna ab initio simulation package (VASP) program.[3] Khon–Sham orbitals were expanded with a cutoff energy of 400.0 eV, and 2 × 2 × 1 equally spaced *k*-point grids were used for Brillouin zone sampling in structural relaxation and electronic structure calculations, respectively.[4]

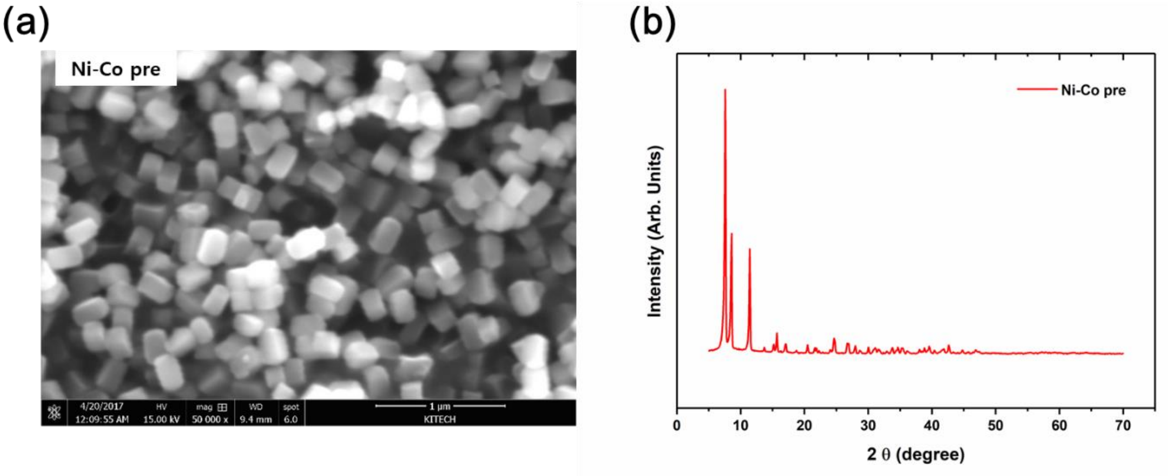

Figure S1. (a) SEM image and (b) XRD pattern of Ni-Co precursors.

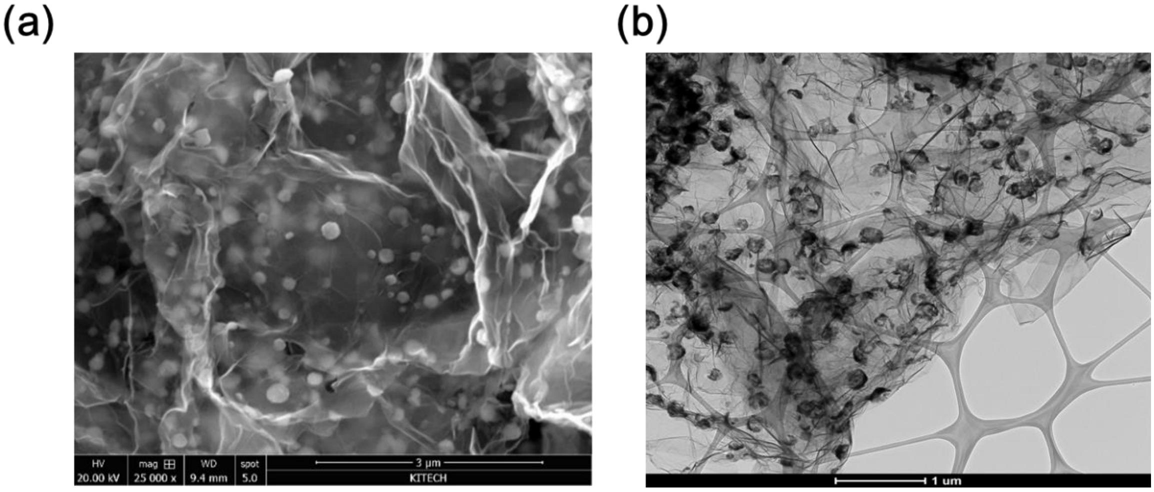

Figure S2. (a) SEM and (b) low-resolution TEM images of CNS-rGO.

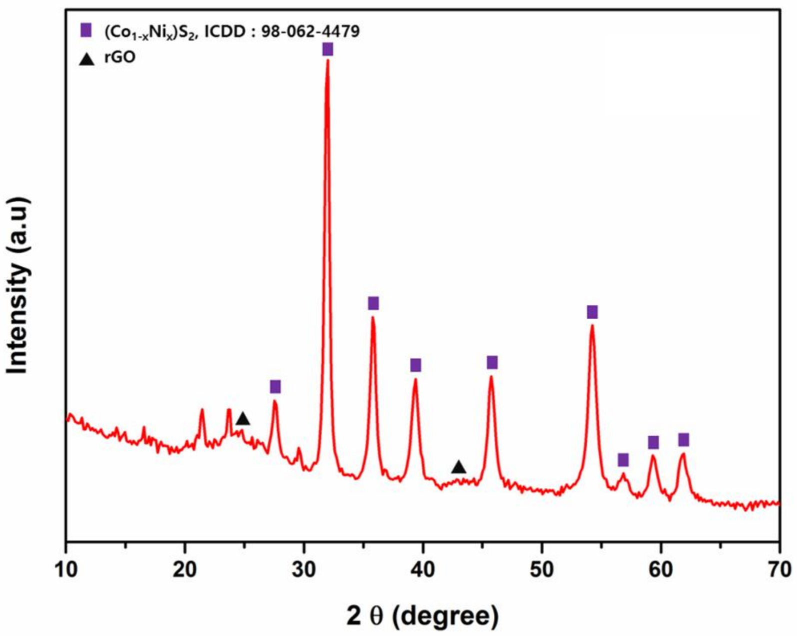

Figure S3. XRD patterns of CNS-rGO.

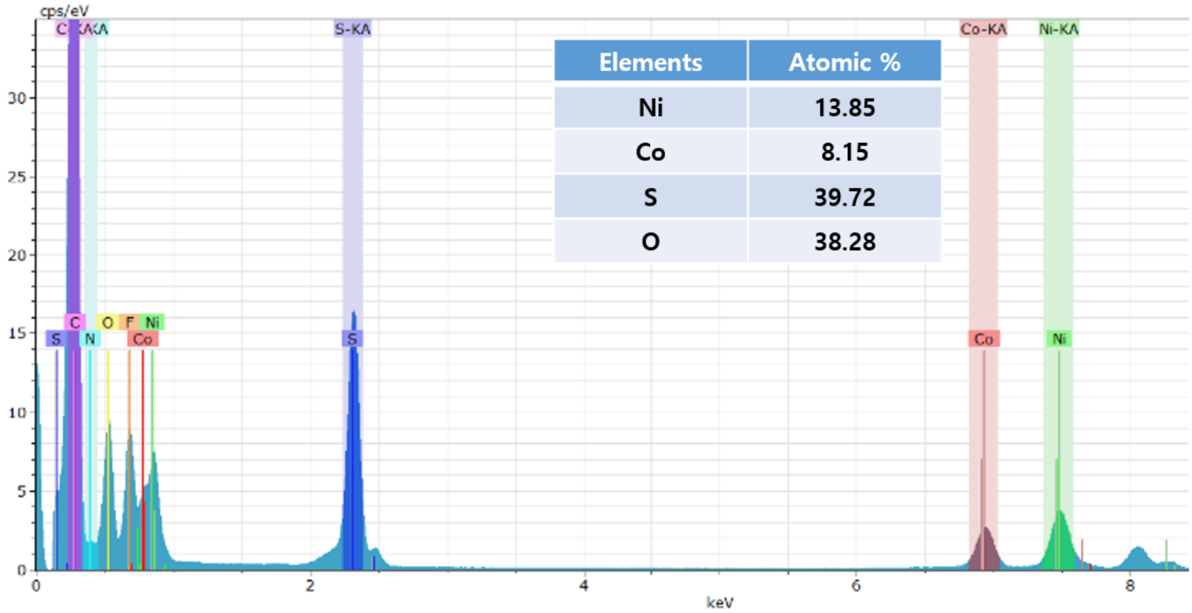

Elements	Atomic %
Ni	13.85
Co	8.15
S	39.72
O	38.28

Figure S4. Quantitative analysis on EDS mapping data of ECA-CNS.

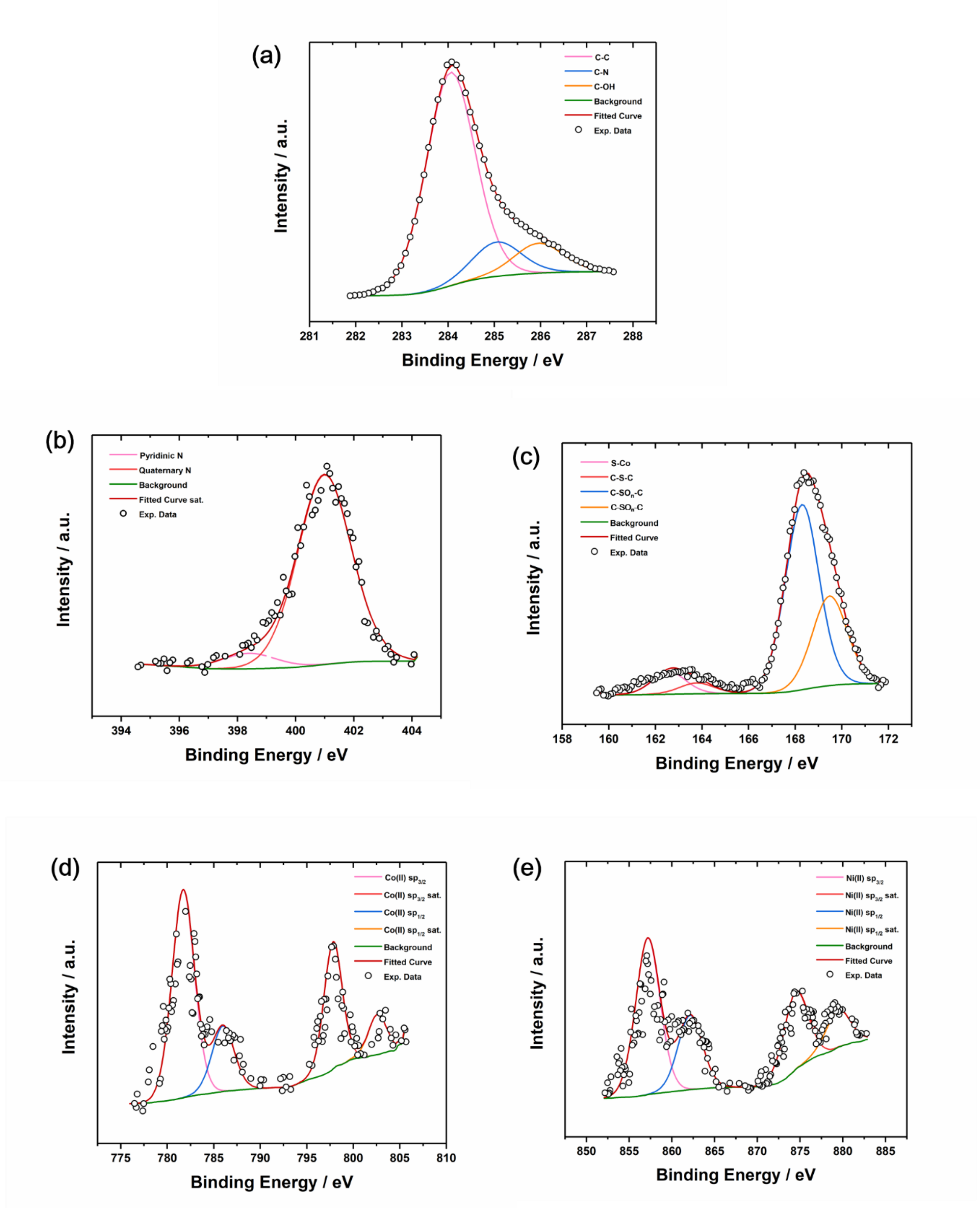

Figure S5. XPS spectra of ECA-CNS sample for (a) C 1s, (b) N 1s, (c) S 2p, (d) Co 2p 1s, and (e) Ni 2p.

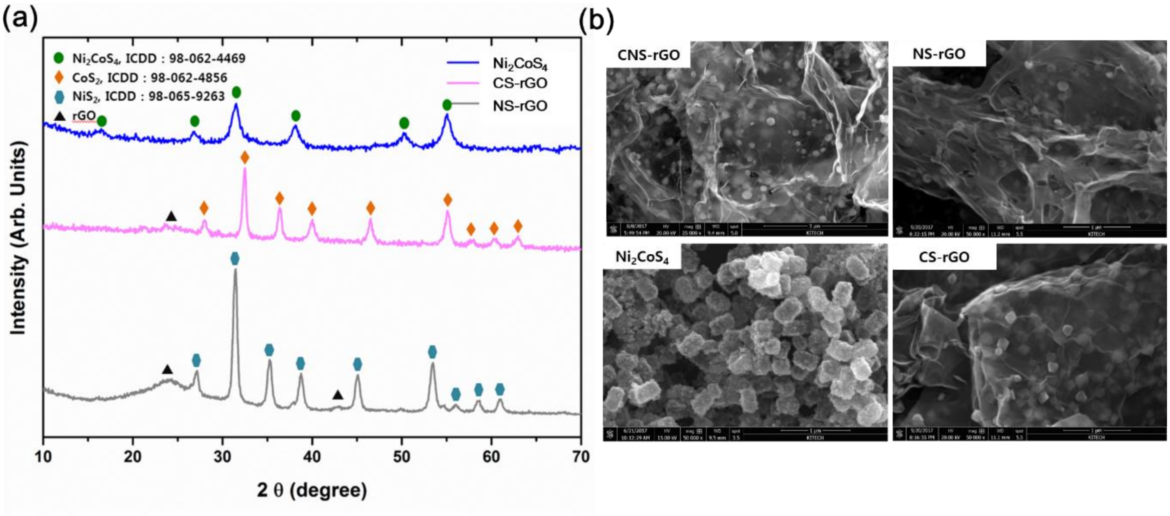

Figure S6. (a) XRD patterns of Ni_2CoS_4, CS-rGO, and NS-rGO. (b) SEM images of CNS-rGO, Ni_2CoS_4, CS-rGO, and NS-rGO.

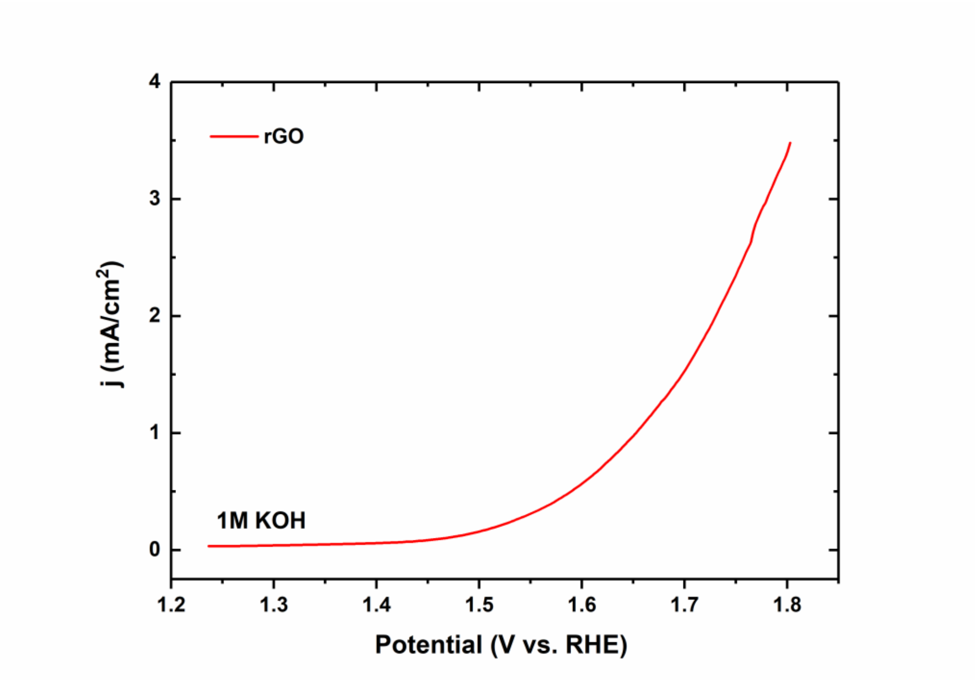

Figure S7. LSV curve of rGO in 1M KOH solution.

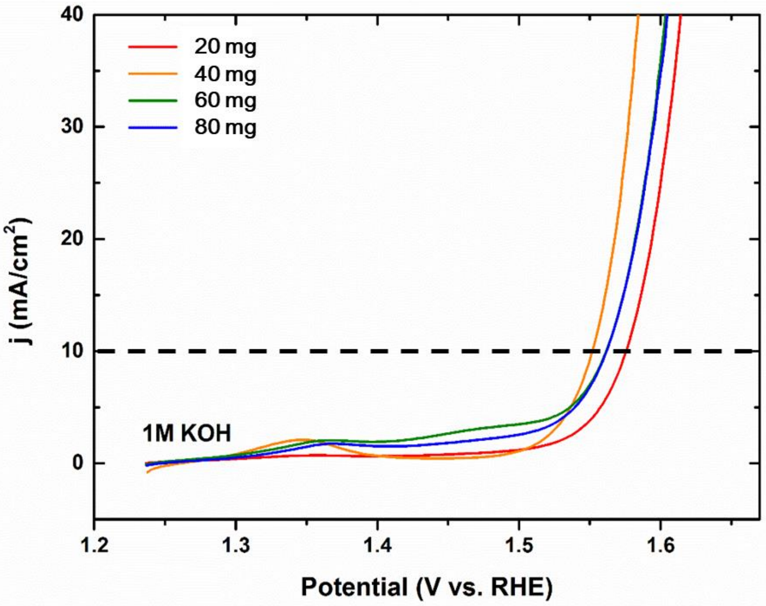

Figure S8. LSV curve of CNS-rGO with different loading of Ni-Co precursor in 1M KOH solution.

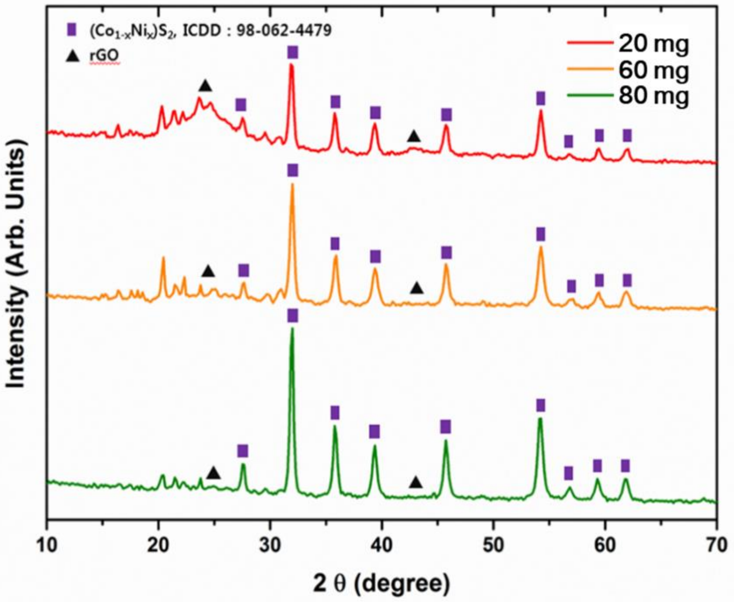

Figure S9. XRD patterns of CNS-rGO with different loading of Ni-Co precursor.

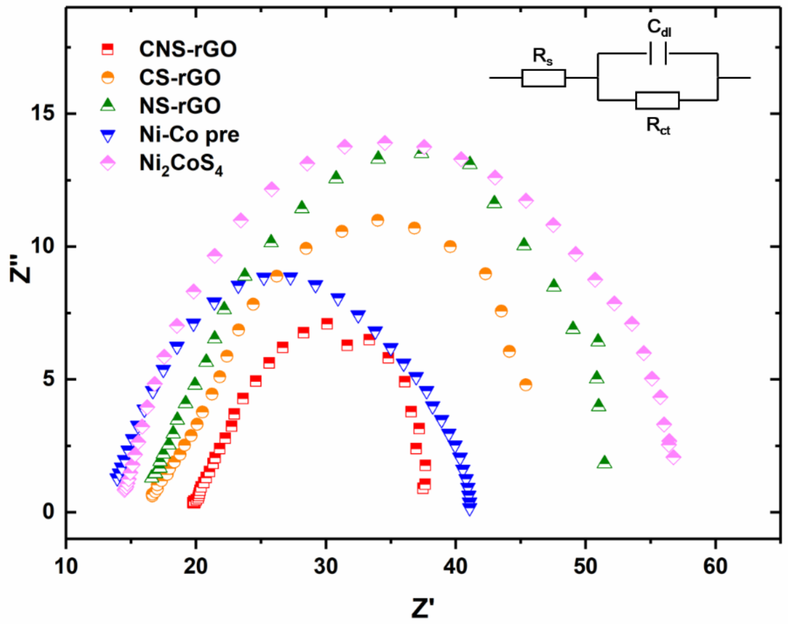

Figure S10. Nyquist plots of CNS-rGO, CS-rGO, NS-rGO, Ni-Co precursor, and Ni_2CoS_4 measured in a frequency range from 0.1 to 100 kHz.. A sinusoidal voltage with an amplitude of 5 mV was applied.

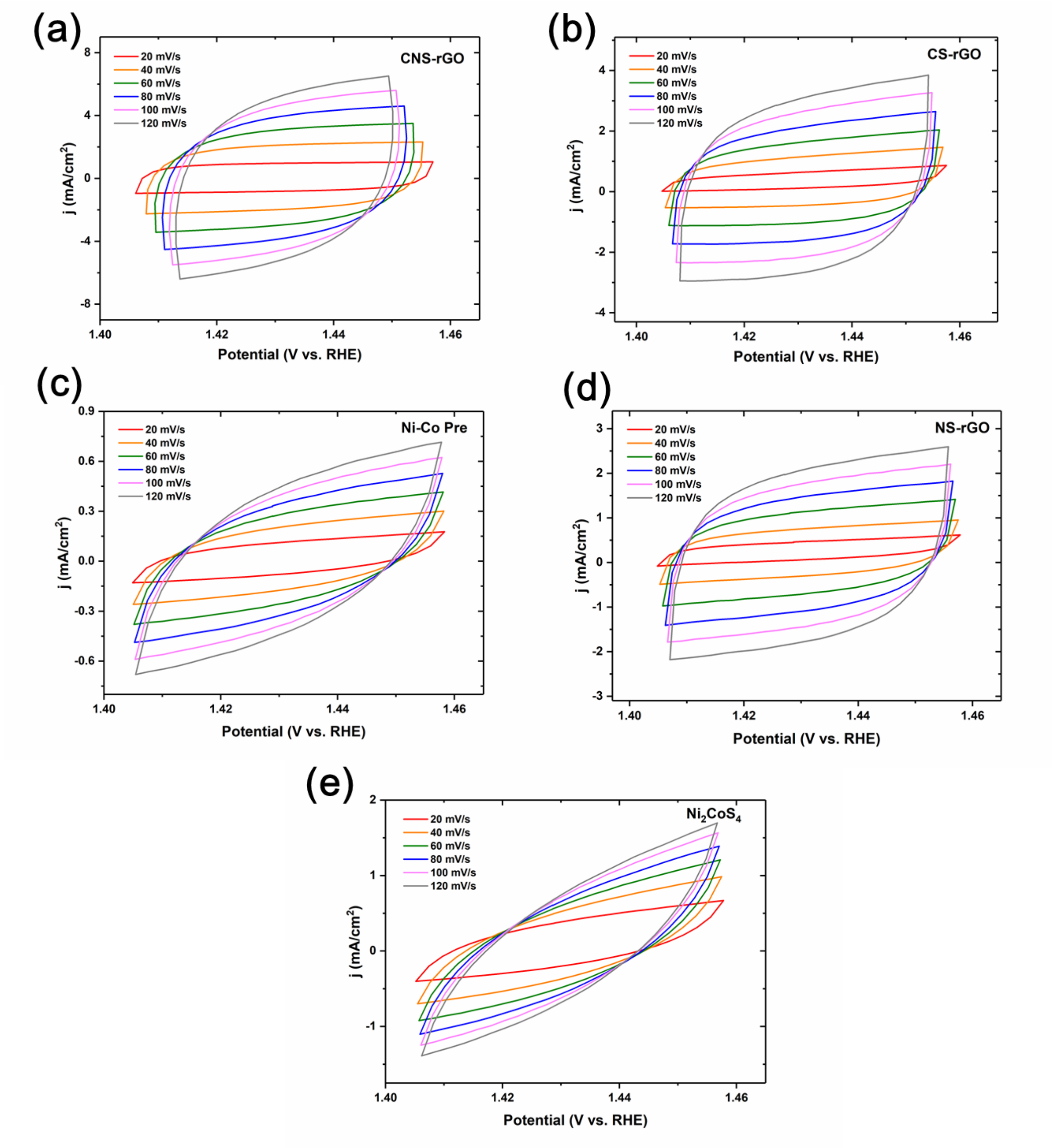

Figure S11. CV measurements in a voltage range of 1.4 – 1.46 V_{RHE} at scan rates 20, 40, 60, 80, 100, and 120 mV s^{-1} of (a) CNS-rGO, (b) CS-rGO, (c) Ni-Co precursor, (d) NS-rGO, and (e) Ni_2CoS_4.

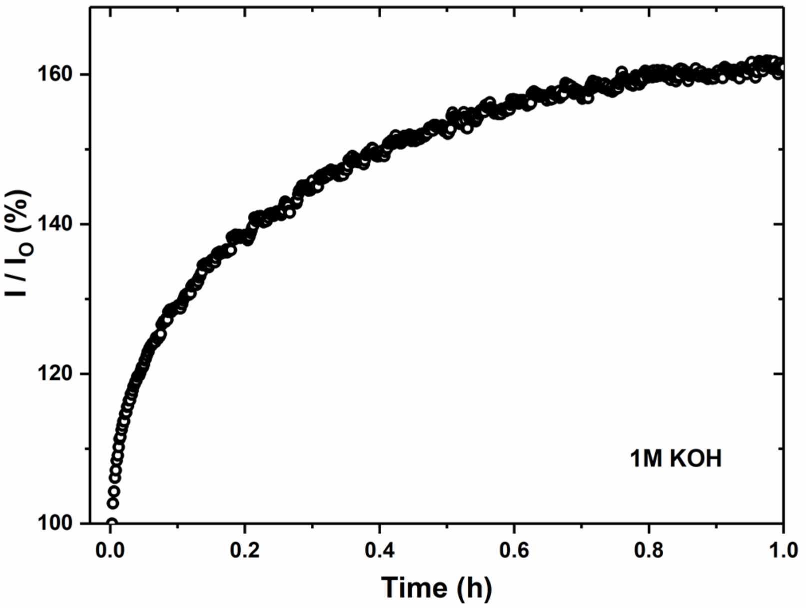

Figure S12. Typical chronoamperometry for CNS-rGO during ECA process in 1M KOH.

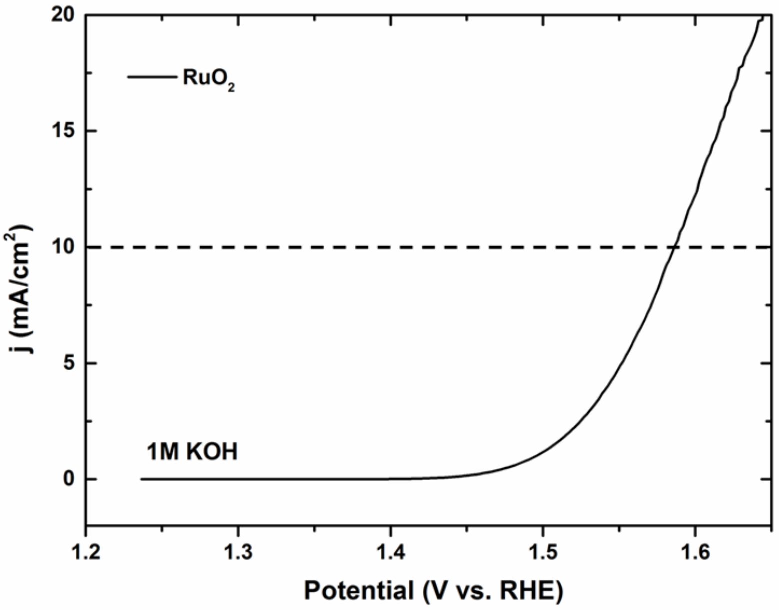

Figure S13. LSV curve of RuO_2 in 1 M KOH.

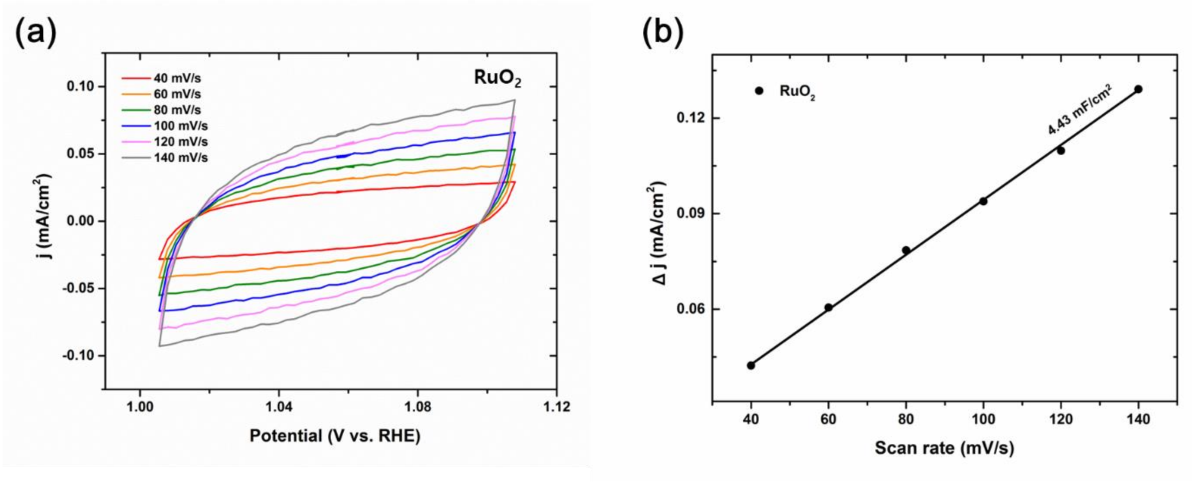

Figure S14. CV measurements in a voltage range of 1.0 – 1.12 V_{RHE} at scan rates 40, 60, 80, 100, 120, and 140 mV s^{-1} of (a) RuO_2 and (b) the calculated ECSA.

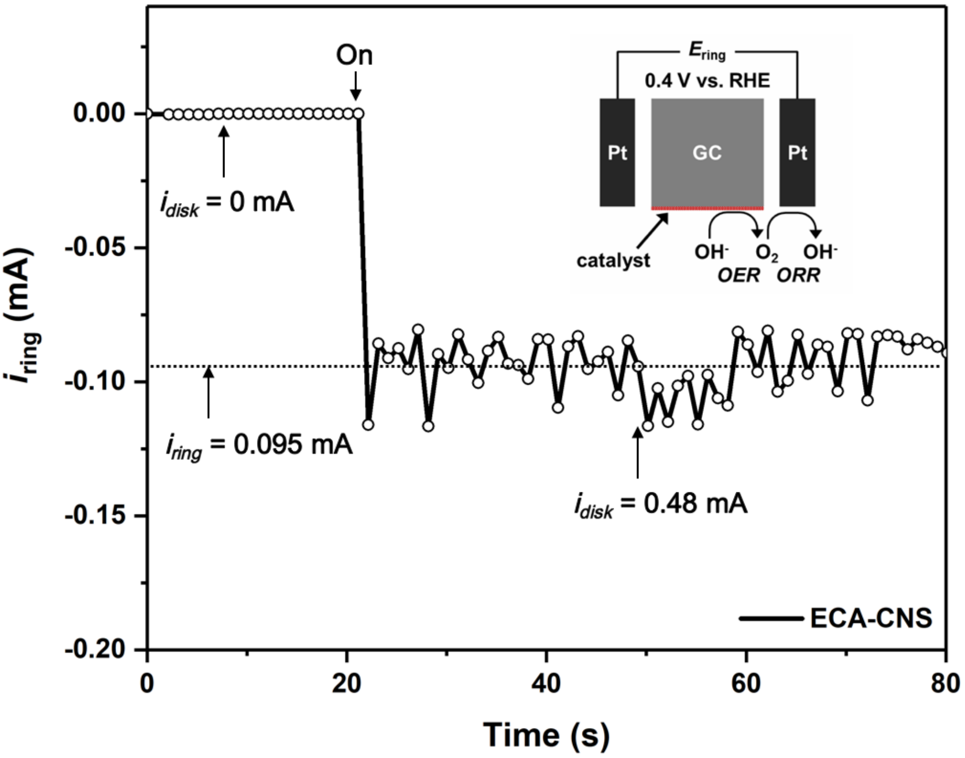

Figure S15. RRDE data for ECA-CNS and the inset shows the schematic setting of the RRDE measurement.

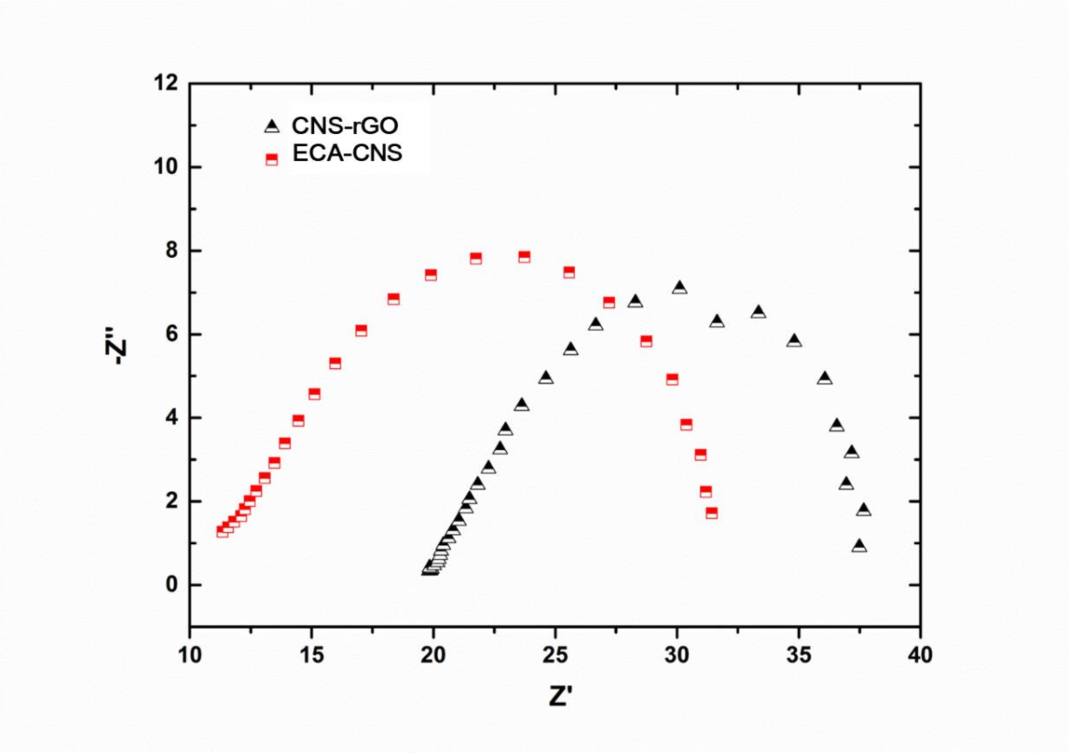

Figure S16. Nyquist plots of CNS-rGO and ECA-CNS measured in a frequency range from 0.1 to 100 kHz.. A sinusoidal voltage with an amplitude of 5 mV was applied

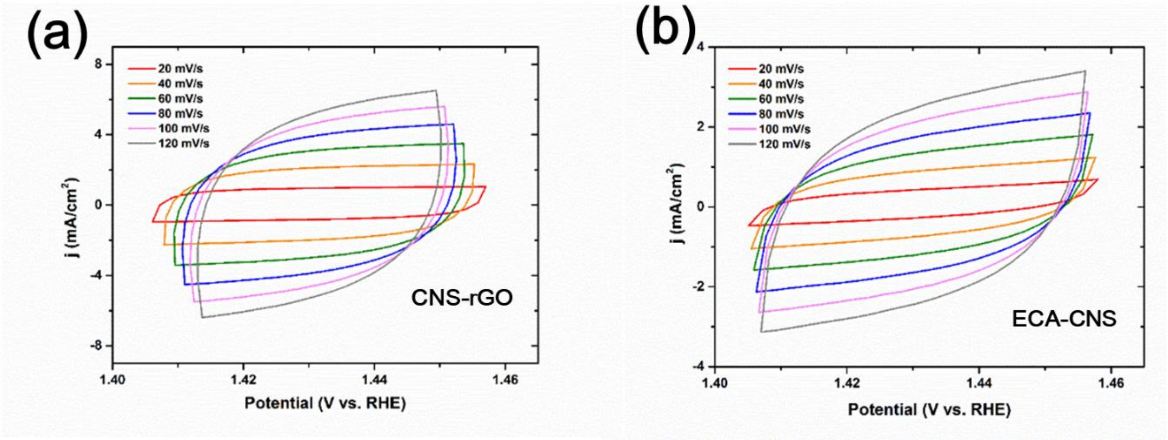

Figure S17. CV measurements in a voltage range of 1.4 – 1.46 V_{RHE} at scan rates 20, 40, 60, 80, 100, and 120 mV s^{-1} of (a) CNS-rGO and (b) ECA-CNS.

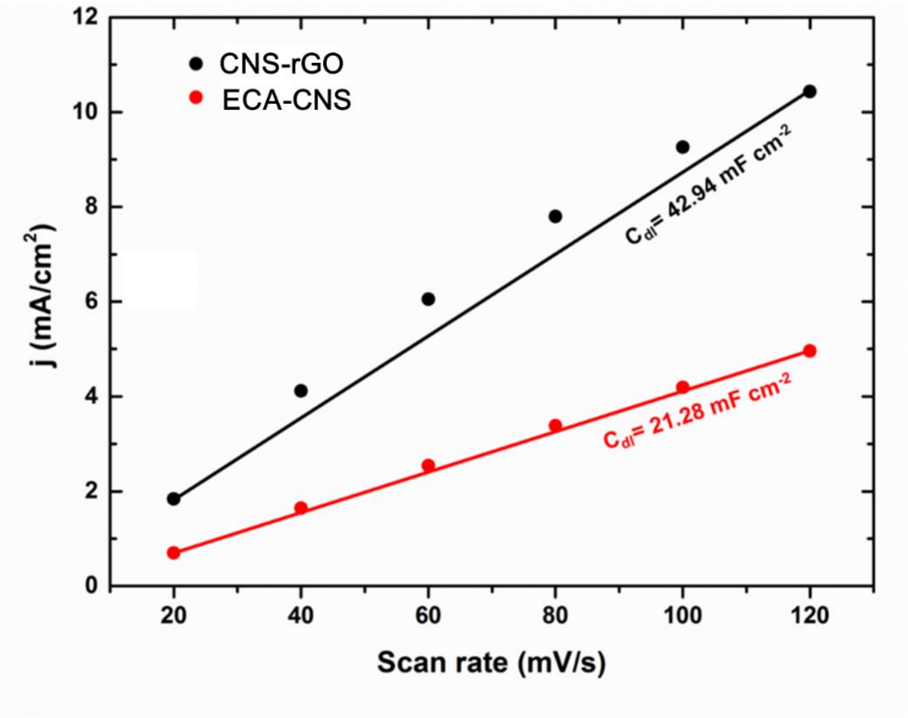

Figure S18. Calculated ECSA of CNS-rGO and ECA-CNS.

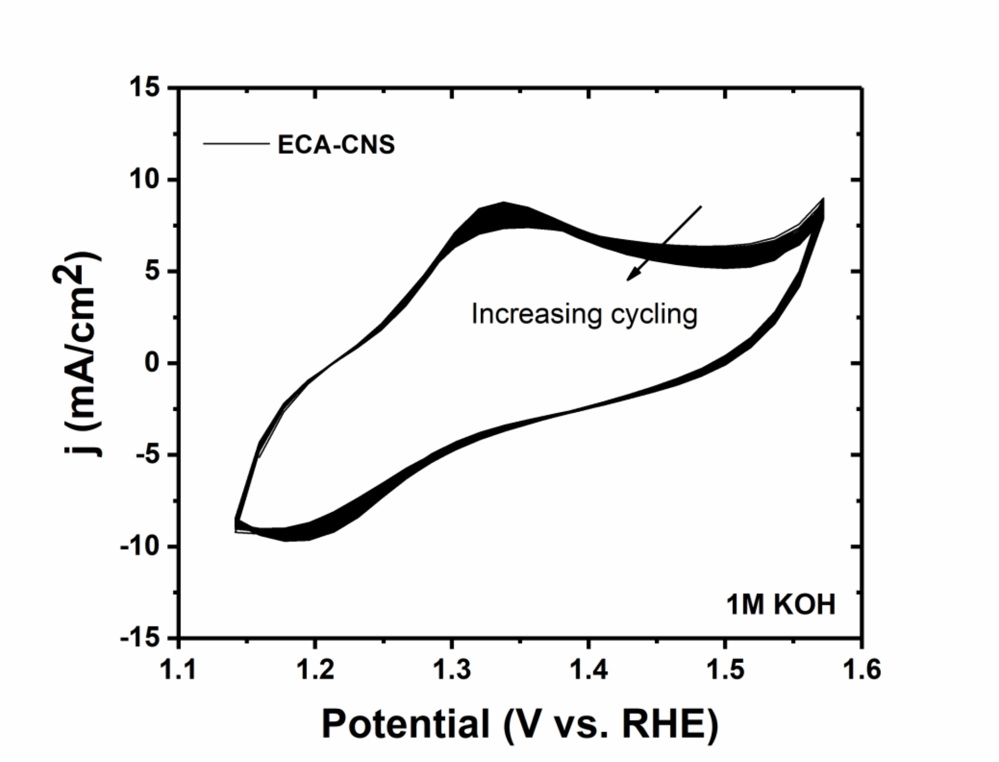

Figure S19. Continuous potential cycling between 1.15 and 1.55 V at 100 mVs^{-1} in 1.0 M KOH.

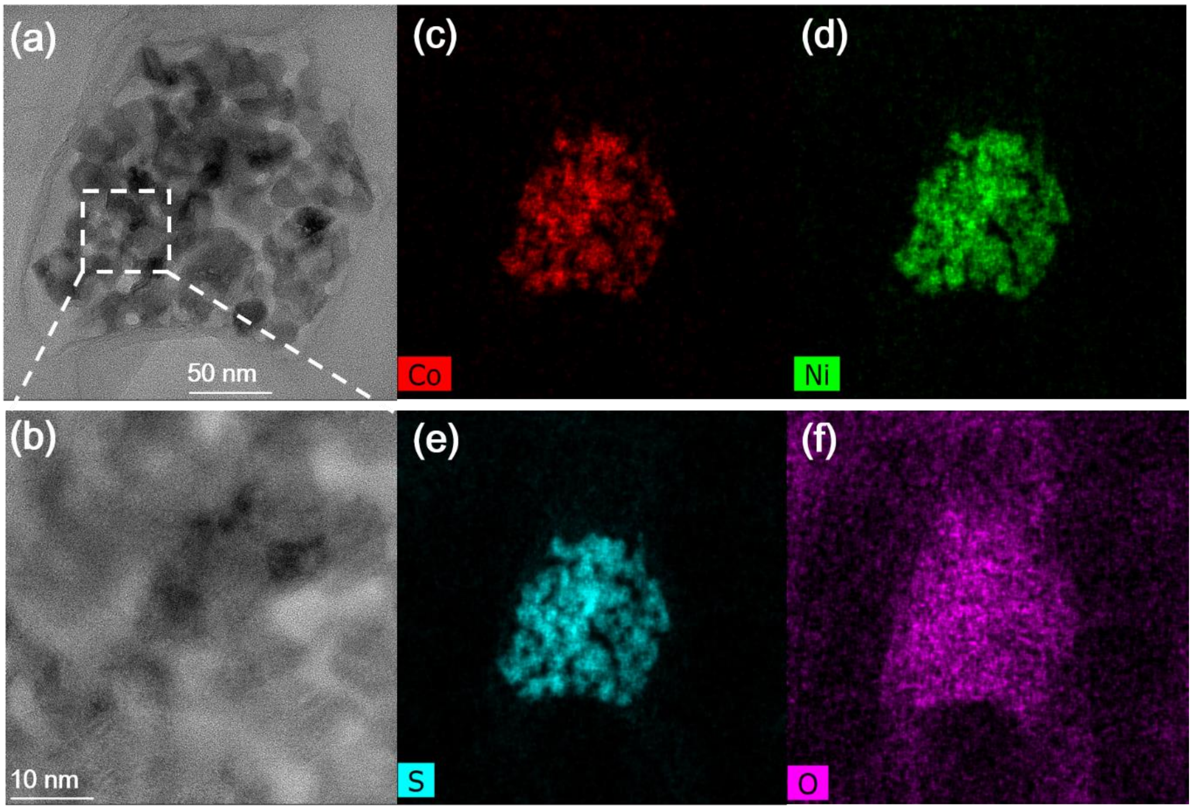

Figure S20. (a) Low-resolution and (b) high-resolution TEM images of ECA-CNS after 10 h long-term OER test. (c-f) Corresponding elemental (Co, Ni, S, and O) mapping images.

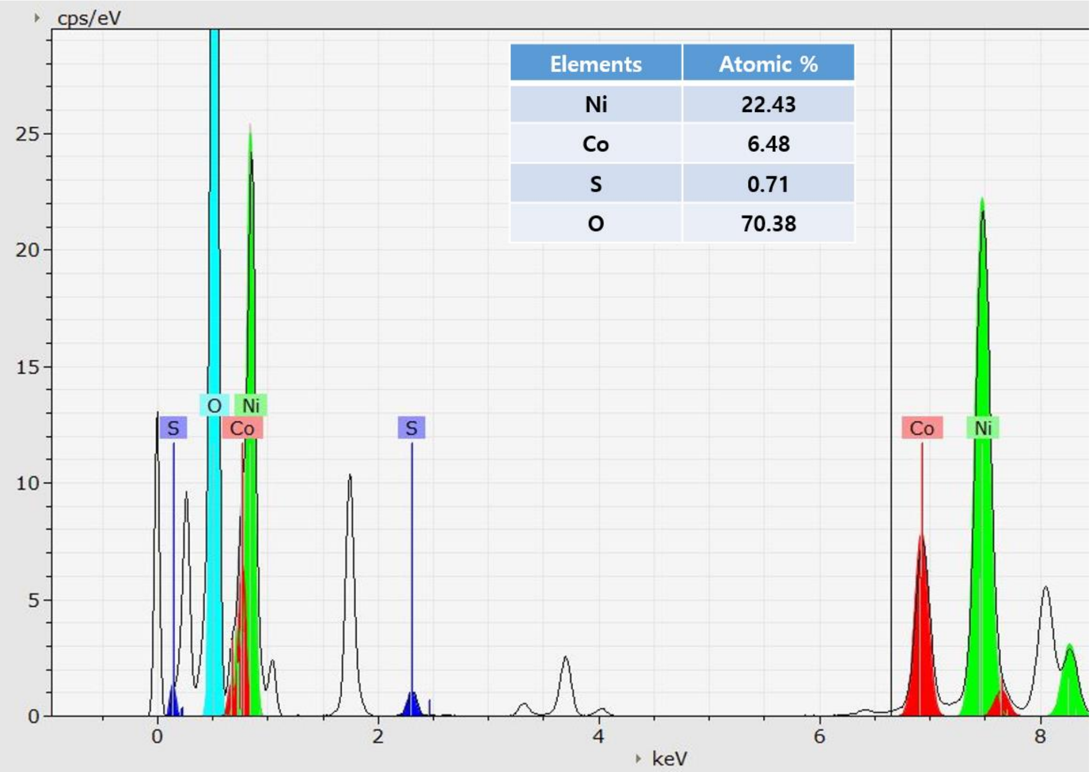

Elements	Atomic %
Ni	22.43
Co	6.48
S	0.71
O	70.38

Figure S21. Quantitative analysis on EDS mapping data of ECA-CNS after long-term OER.

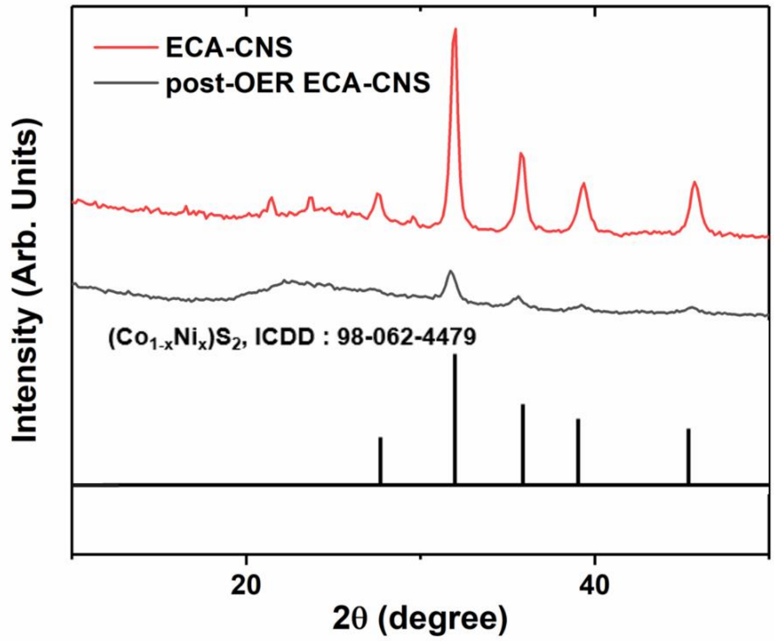

Figure S22. XRD patterns for ECA-CNS before and after long-term OER test for 10 hrs in 1.0 M KOH.

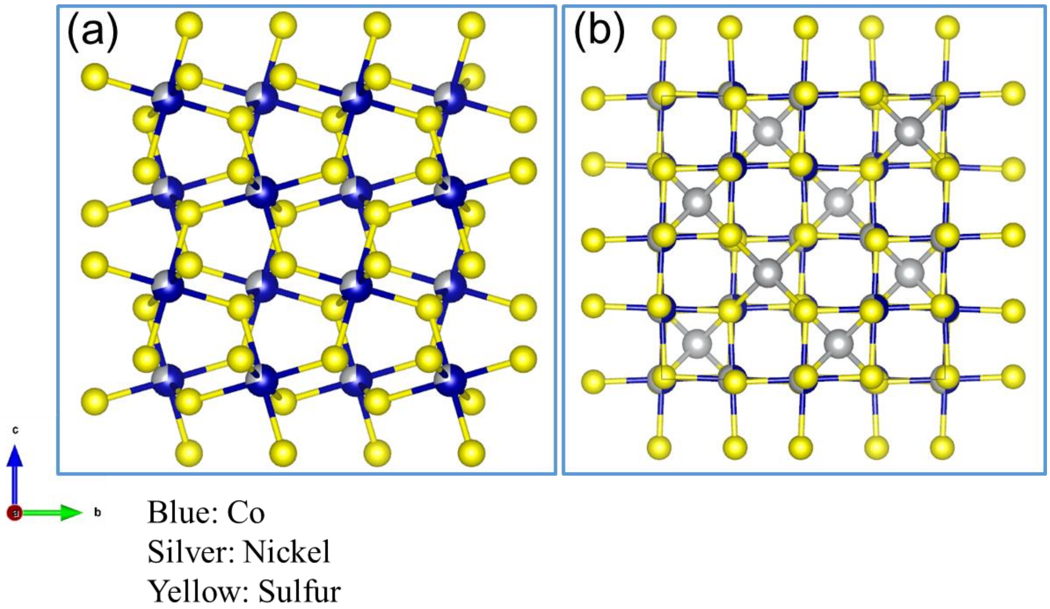

Figure S23. Crystal structures of (a) $CoNiS_4$ and (b) Ni_2CoS_4 are shown where yellow, blue, and silver colors represent oxygen, cobalt, and nickel atoms. Ni atoms in Ni_2CoS_4 are bonded with S atoms in both tetrahedral and octahedral coordination

Table S1. Comparison of OER catalytic activity of ECA-CNS with reported state of the art OER electrocatalysts on glassy carbon (GC) electrode in alkaline media.

Catalysts	Electrolyte	η^{10} (mV)	Tafel slope (mV dec^{-1})	References
ECA-CNS	1 M KOH	290	46	This work
CoxOy/NC	0.1 M KOH	430	75	*Angew. Chem. Int. Ed.* 2014, *53*, 8508
Co3O4/r-GO	1 M KOH	310	67	*Nat. Mater.* 2011, *10*, 780
Co-CoO/N-rGO	0.1 M KOH	~400	68	*Adv. Funct. Mater.* 2015, *25*, 5799
Co_9S_8@MoS_2/CNFs	1 M KOH	430	61	*Adv. Mater.* 2015, *27*, 4752
NG-CNT	0.1 M KOH	520	141	*Adv. Mater.* 2014, *26*, 2925.
CoMn LDH	1 M KOH	324	43	*J. Am. Chem. Soc.* 2014, *136*, 16481
NiCoS/CC NSs	1 M KOH	330	109	*Int. J. Hydrogen Energy 2015, 40, 4727*
$NiCo_2S_4$ NA/CC	1 M KOH	340	89	*Nanoscale 2015, 7, 15122*
NiSe/NF	1 M KOH	400	N/A	*Angew. Chem., Int. Ed. 2015, 54, 9351*
CP@FeP	1 M KOH	365	63	*Chem. Commun. 2016, 52, 8711*

Reference for SI

[1] J. P. Perdew, K. Burke, M. Ernzerhof, *Phys Rev Lett* 1997, 78, 1396.

[2] J. P. Perdew, K. Burke, M. Ernzerhof, *Phys Rev Lett* 1997, 78, 1396.

[3] G. Kresse, *J Non-Cryst Solids* 2002, 312-14, 52.

[4] R. A. Evarestov, V. P. Smirnov, *Phys Rev B* 2004, 70.